ISSN 1063-7710, Acoustical Physics, 2020, Vol. 66, No. 5, pp. 461–468. © Pleiades Publishing, Ltd., 2020.

CLASSICAL PROBLEMS OF LINEAR ACOUSTICS AND WAVE THEORY

Reflection of Plane Waves at an Interface of Water/Patchy Saturated Porous Media with Underlying Solid Substrate

Puyi Li[a], Lina Gao[a], Jinxia Liu[a], Zhengliang Cao[b], and Zhiwen Cui[a, *]

[a] *Department of Acoustics and Microwave Physics, College of Physics, Jilin University, Changchun, 130012 China*

[b] *Shanghai Engineering Research Center of Hadal Science and Technology, College of Marine Sciences, Shanghai Ocean University, Shanghai, 201306 China*

**e-mail: cuizw@jlu.edu.cn*

Received December 4, 2018; revised March 3, 2020; accepted April 28, 2020

Abstract—The problems with elastic wave reflection at the interface between the water/patchy saturated porous media and the underlying solid matrix are considered. When porous media is saturated by biphasic fluids, the patchy saturation theory can explain the wave dispersion and attenuation better than the classical Biot theory at mesoscopic scales. Based on patchy saturation theory, this paper focuses on the reflection of elastic waves by patchy saturated porous media inclusion in layered media. Using numerical calculation, the reflection coefficients with different excitation frequencies, water saturations, and porous media depths are discussed. The results show that the differences between two kinds of patchy saturated porous media cases in the oil-water model are lower than those between the same two cases in the gas-water model. Low water saturation and high water saturation have significant effects on the reflection coefficient.

Keywords: patchy saturation, water, underlying solid, reflection coefficients, elastic waves

DOI: 10.1134/S1063771020050085

1. INTRODUCTION

The reflection–refraction phenomena of elastic waves from the interface between two elastic media play an important role in modern seismology from both theoretical and practical points of view. These problems have extensive and wide applications in petroleum engineering, exploration geophysics, building industry and various other fields. When a seismic wave propagates through two different media, the reflection and refraction phenomena take place. These reflected and refracted waves from the interface carry lots of information about the characteristics of the media. The records of seismic signals are beneficial for determining the different physical properties of the Earth' s medium. A mass of literature is available on the theories and experiments performed to study the problems of reflection and refraction of seismic waves by considering different models. Stoll and Kan [1] investigated the reflection when a plane wave was incident to porous sediment from water based on the Biot theory. Cui and Wang [2] used the BISQ model to study the influence of the squirt flow on reflection and refraction of elastic waves at a fluid/fluid-saturated porous solid interface. Tajuddin et al. [3] studied the reflection of plane waves at the boundaries of a liquid-filled poroelastic half-space. Markov [4–6] did a lot of research about wave-propagation in fluid-saturated porous media. He [4] studied the propagation of P-wave in a fluid-saturated porous media with spherical inclusions. He [5] investigated Rayleigh wave propagation along the boundary of a non-Newtonian fluid-saturated porous media. Markov [6] researched the reflection of elastic waves at an interface between two porous half-space filled with two different fluids.

Many researchers focus on the fluid-saturated porous media, while it is well known that the Earth is composed of complex media. Dunin et al. [7] and Nikolaevskiĭ et al. [8] studied nonlinear waves and the acoustic action in porous media saturated with "live" oil. Some researchers applied various methods to investigate the reflection coefficient of porous media saturated by multiple fluids. Zhijun Dai et al. [9] investigated the reflection and transmission of elastic waves at the interface between an elastic solid and a double porosity medium. Wang et al. [10] and Lyu et al. [11] investigated wave propagation at the porous sediment interface with a solid substrate and double-porosity substrate, respectively. Weiyun Chen et al. [12] analyzed the influences of layer thickness, incident angle, wave frequency and liquid saturation of sandwiched porous layer on the reflection coefficient of the acoustic wave from the elastic seabed with an overlying gassy poroelastic layer. The sandwiched gassy poroelastic medium is considered as a mixture consisting of a deformable solid frame, a liquid phase, and a gas phase.

When rocks are partially saturated with two different fluids, a physics model of patchy saturation was presented by Dutta and Odé [13, 14] and Dutta and Seriff [15] reformulated White's model and made several corrections to the initial White's model. Other revisions and verifications to White's model have also been developed by Gist [16] and Johnson [17]. Johnson [17] developed the patchy-saturation model and consummated the patchy saturation theory. The theory assumes that one fluid phase with higher mobility is a sphere surrounded by another less mobile fluid in a porous medium. Pride [18] and Berryman [19] developed patchy saturated composites with two isotropic porous constituents and derived the frequency and material-property dependencies of the internal transport coefficient which controls the mesoscopic fluid-pressure equilibration between the two porous constituent phases. Then the patchy saturation theory allows using the framework of Biot-Gassmann via some generalized frequency-dependent parameters [20]. Abrashkin et al. [21] provided a possible mechanism of the acoustic action on partially fluid-saturated porous media. They presented a theoretical description of both situations: with and without considering the viscous effects and they performed a numerical study of the drop motion in cylindrical, conic, and corrugated capillaries. Tomar et al. [22] investigated the reflection and transmission of elastic waves at an elastic/porous solid saturated by two immiscible fluids using the theory proposed by Tuncay and Corapcioglu [23]. Quintal [24] studied the impact of changes in the saturation on the frequency-dependent reflection coefficient of a partially saturated layer by using the analytical solution of the 1D White's model.

Some scientists have investigated seismic wave attenuation and velocity dispersion in partially saturated rocks [18, 19, 25–28]. Müller et al. [25] investigated the attenuation and dispersion of elastic waves for 3D patchy saturated rocks by using the results of Müller and Gurevich [26] and Toms et al. [27]. Dupuy and Stovas [28] calculated seismic wave velocity dispersion and attenuation in partially saturated gas-water and oil-water reservoirs and compared the patchy saturation results with results coming from the upscaling theory.

In this paper, we use the patchy saturation theory which involves frequency-dependent parameters in a generalized Biot–Gassmann formalism [19] to study the reflection of elastic waves at an interface of water/patchy saturated porous media with an underlying solid substrate. In the presented work, we calculate the reflection coefficients with various excitation frequencies, water saturations, patchy saturated porous media depths and biphasic fluids in the porous media. The goal of this paper is to provide help to explore oil and natural gas resources theoretically in porous sediment or other geological conditions.

2. PATCHY SATURATION THEORY AND FIELD EQUATIONS FOR PATCHY SATURATED POROUS

Based on Biot theory about saturated porous media, Pride et al. formulated dynamic equations which govern particle motions in the frequency domain, assuming a time dependency in $e^{-i\omega t}$, as

$$\begin{aligned}\boldsymbol{\tau} &= \left[K_U(\omega)\nabla\cdot\mathbf{u} + C(\omega)\nabla\cdot\mathbf{w}\right]\mathbf{I}\\ &+ G(\omega)\left[\nabla\mathbf{u} + (\nabla\mathbf{u})^T - 2/3\,\nabla(\mathbf{uI})\right],\\ -P &= C(\omega)\nabla\cdot\mathbf{u} + M(\omega)\nabla\cdot\mathbf{w},\\ \nabla\cdot\boldsymbol{\tau} &= -\omega^2(\rho\mathbf{u} + \rho_f\mathbf{w}),\\ -\nabla P &= -\omega^2(\rho_f\mathbf{u} + \tilde{\rho}\mathbf{w}),\end{aligned} \tag{1}$$

where $\mathbf{u}$ is the solid displacement. The relative fluid/solid displacement is $\mathbf{w} = (\mathbf{u_f} - \mathbf{u})$, φ is porosity and $\mathbf{u_f}$ is the fluid displacement,τ and P denote the stress tensor and the fluid pressure and $\mathbf{I}$ is a unit tensor. The fluid density, the total density and the flow resistance terms are denoted by ρ_f, and $\tilde{\rho}$, respectively. The bulk modulus $K_U(\omega)$, the Biot modulus $C(\omega)$, the storage coefficient $M(\omega)$ and the shear modulus $G(\omega)$ are frequency-dependent which describe the complex porous medium and the fluid behavior of the effective porous medium [19].

To use the generalized Biot–Gassmann theory, Pride et al. [19] built an effective porous medium according to the properties of partially saturated medium. The drained bulk modulus $K_D(\omega)$, the undrained bulk modulus $K_U(\omega)$ and the Skempton modulus $B(\omega)$ of the porous composite are formulated by Pride as

$$\frac{1}{K_D(\omega)} = a_{11} - \frac{a_{13}^2}{a_{33} - \gamma(\omega)/i\omega}, \tag{2}$$

$$B(\omega) = \frac{-a_{12}(a_{33} - \gamma(\omega)/i\omega) + a_{13}(a_{23} + \gamma(\omega)/i\omega)}{(a_{22} - \gamma(\omega)/i\omega)(a_{33} - \gamma(\omega)/i\omega) - (a_{23} + \gamma(\omega)/i\omega)^2}, \tag{3}$$

$$\frac{1}{K_U(\omega)} = \frac{1}{K_D(\omega)} + B(\omega)\left(a_{12} - \frac{a_{13}(a_{23} + \gamma(\omega)/i\omega)}{a_{33} - \gamma(\omega)/i\omega}\right). \quad (4)$$

The internal transport coefficient $\gamma(\omega)$ is given by Pride et al [19]. This coefficient describes the behavior law of fluid transfers which depends on capillarity effects and on interphase mesoscopic flows. The a_{ij} $(i, j \in (1,3))$ are real elastic compliances which are related to the elastic moduli of the two fluids (see [19] for details). Then the complex moduli $C(\omega)$ and $M(\omega)$ are given by

$$C(\omega) = B(\omega)K_U(\omega), \quad (5)$$

$$M(\omega) = C(\omega)/\alpha, \quad (6)$$

where α is Biot–Willis constant. $G(\omega)$ is assumed to be frequency-independent in the seismic frequency band and equal to the drained shear modulus G where squirt flow mechanisms are negligible [15].

By Helmholtz representation of vectors, the displacement vectors $\mathbf{u}$ and $\mathbf{w}$ can be written as

$$\mathbf{u} = \nabla\varphi_{P1} + \nabla\varphi_{P2} + \nabla \times \boldsymbol{\psi}, \quad (7)$$

$$\mathbf{w} = \alpha_{P1}\nabla\varphi_{P1} + \alpha_{P2}\nabla\varphi_{P2} + \alpha_S\nabla \times \boldsymbol{\psi}, \quad (8)$$

where φ_{P1} and φ_{P2} are scalar displacement potentials, $\boldsymbol{\psi}$ is vector displacement potential. α_{P1}, α_{P2} and α_S, the amplitude ratio of the solid skeleton potential to the pore fluid increment potential, are given by

$$\alpha_i = -\frac{H(\omega)s_i^2 - \rho}{C(\omega)s_i^2 - \rho_f}, \quad i = p1, p2, \quad (9)$$

$$\alpha_S = \frac{G(\omega)}{\rho}\left(s_S^2 - \frac{\rho}{G(\omega)}\right), \quad (10)$$

where

$$s_{p1,p2}^2 = \frac{\gamma}{2} \mp \sqrt{\left(\frac{\gamma}{2}\right)^2 - \frac{\tilde{\rho}\rho - \rho_f^2}{H(\omega)M(\omega) - C^2(\omega)}}, \quad (11)$$

$$\gamma = \frac{\rho M(\omega) + \tilde{\rho}H(\omega) - 2\rho_f C(\omega)}{H(\omega)M(\omega) - C^2(\omega)}, \quad (12)$$

the "–" corresponds to the slowness of Biot's fast compressional ($p1$) wave while the "+" corresponds to the slowness of Biot's slow compressional ($p2$) wave. The shear waves (S) slowness is given by

$$s_S^2 = \frac{1}{G(\omega)}\left(\rho - \frac{\rho_f^2}{\tilde{\rho}}\right). \quad (13)$$

In the theory of [19] there are two approximate methods in two cases depending on the fluid proportions. One case is that the proportion of phase 1 is considerably larger than phase 2, the other case is just opposite.

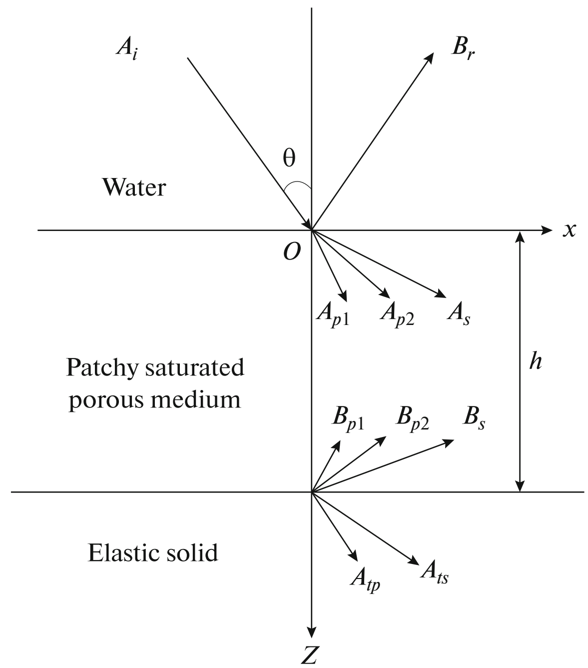

Fig. 1. Physical model of the water-patchy saturated porous medium: elastic solid system with a plane wave incident from the water.

When the proportions of phase 1 and phase 2 have the same order in magnitude, we can not deduce analytic solutions. However the patchy saturation theory is more efficient and applicable to some questions in the framework of Biot model. Therefore, the following discussion will focus on the two cases mentioned before using the patchy saturation theory [19].

3. PROBLEM FORMULATION AND BOUNDARY CONDITIONS

3.1. Formulations of Reflection and Refraction Problem

In this paper, the analyzed system includes overlying water, a patchy saturated porous media layer and a solid substrate below, as shown in Fig. 1. Using a Cartesian system with the x-axis rightward and z-axis downward, $z = 0$ and $z = h$ represent the interfaces separating the water, the porous medium, and the solid substrate, respectively. When a compressible plane wave strikes at the patchy saturated porous media interface from the water, there will generate reflected P-wave in the water, transmitted and refracted $p1$-wave, $p2$-wave, and S-wave in porous media and transmitted P- and S- waves in the underlying solid. And incident angle, excitation frequency, porous media depth and water saturation (the proportion of water) are denoted by, f, h and S_1, respectively.

The scalar displacement potential of the water ($z < 0$) is given by:

$$\varphi_w = A_i e^{i(l_i x + \sigma_i z)} + B_r e^{i(l_i x - \sigma_i z)}, \tag{14}$$

where A_i and B_r denote the amplitude; l_i and σ_i denote the x- and z-components of the wave number, respectively.

The displacement potentials of porous media ($0 < z < h$) are given by:

$$\varphi_{p1} = A_{p1} e^{i(l_{p1} x + \sigma_{p1} z)} + B_{p1} e^{i(l_{p1} x - \sigma_{p1} z)}, \tag{15}$$

$$\varphi_{p2} = A_{p2} e^{i(l_{P2} x + \sigma_{P2} z)} + B_{p2} e^{i(l_{P2} x - \sigma_{P2} z)}, \tag{16}$$

$$\psi = A_s e^{i(l_s x + \sigma_s z)} + B_s e^{i(l_s x - \sigma_s z)}, \tag{17}$$

where A_{p1}, A_{p2}, A_s, B_{p1}, B_{p2} and B_s denote the amplitude; l_{p1}, l_{p2}, l_s and σ_{p1}, σ_{p2}, σ_s denote the x- and z-components of the wave number, respectively.

The motion equation of elastic solid is given by

$$(\lambda_e + \mu_e)\nabla\nabla\mathbf{u}' + \mu_e \nabla^2 \mathbf{u}' = \rho_e \ddot{\mathbf{u}}', \tag{18}$$

where λ_e and μ_e are Lame's constants, ρ_e denotes the solid density, and $\mathbf{u}'$ is the displacement vector.

Based on the Helmholtz theorem, the displacement vector $\mathbf{u}'$ can be written as

$$\mathbf{u}' = \nabla\varphi_e + \nabla \times \boldsymbol{\psi}_e, \tag{19}$$

where φ_e and $\boldsymbol{\psi}_e$ are the scalar and vector displacement potentials, respectively. Thus the x- and z-components of $\mathbf{u}'$ are expressed as follows:

$$u'_x = \frac{\partial\varphi_e}{\partial x} - \frac{\partial\psi_e}{\partial z}, \quad u'_z = \frac{\partial\varphi_e}{\partial z} + \frac{\partial\psi_e}{\partial x}. \tag{20}$$

The scalar and vector displacement potentials of elastic solid ($z > h$)are given by :

$$\varphi_e = A_{tp} e^{i(l_{tp} x + \sigma_{tp} z)}, \tag{21}$$

$$\psi_e = A_{ts} e^{i(l_{ts} x + \sigma_{ts} z)}, \tag{22}$$

where A_{tp} and A_{ts} denote the amplitude; l_{tp}, l_{ts} and σ_{tp}, σ_{ts} denote the x- and z-components of the wave number, respectively. The incident wave number components l_i and σ_i are given by

$$l_i = l_w \sin\theta_i, \quad \sigma_i = l_w \cos\theta_i, \tag{23}$$

where $l_w = \omega/V_w$, V_w is the velocity of compressible wave in the water. According to Snell law, the x-component of wave numbers are all equal to l_i, i.e.,

$$l_{p1} = l_{p2} = l_s = l_{tp} = l_{ts} = l_i. \tag{24}$$

3.2. Interface between the Ideal Fluid and Patchy Saturated Porous Media (z = 0)

(1) The continuity of fluid movement in and out of the skeletal frame in normal direction to the interface, $U_z = u_z + w_z$; i.e.,

$$\frac{\partial\varphi_w}{\partial z} = \left(\frac{\partial\varphi_{P1}}{\partial z} + \frac{\partial\varphi_{P2}}{\partial z} + \frac{\partial\psi}{\partial x}\right) + \left(\alpha_{P1}\frac{\partial\varphi_{P1}}{\partial z} + \alpha_{P2}\frac{\partial\varphi_{P2}}{\partial z} + \alpha_S\frac{\partial\psi}{\partial x}\right). \tag{25}$$

(2) The equilibrium of the water pressure p_w and the pore fluid pressure p, $p_w = p$; i.e.,

$$-\rho_0\omega^2\varphi_w = C(\omega)\nabla^2(\varphi_{P1} + \varphi_{P2}) + M(\omega)\nabla^2(\alpha_{P1}\varphi_{P1} + \alpha_{P2}\varphi_{P2}). \tag{26}$$

(3) The equilibrium of normal stress, $-p_w = \tau_{zz}$; i.e.,

$$-\rho_0\omega^2\varphi_w = (H(\omega) - 2G(\omega))\nabla^2(\varphi_{P1} + \varphi_{P2}) + C(\omega)\nabla^2(\alpha_{P1}\varphi_{P1} + \alpha_{P2}\varphi_{P2}) + 2G(\omega)\left[\frac{\partial^2(\varphi_{P1} + \varphi_{P2})}{\partial z^2} + \frac{\partial^2\psi}{\partial x\partial z}\right], \tag{27}$$

where τ_{zz} is the normal component of total stress of the porous media.

(4) The equilibrium of tangential stress, $0 = \tau_{zx}$; i.e.,

$$0 = G(\omega) \times \left[\frac{\partial^2(\varphi_{P1} + \varphi_{P2})}{\partial x\partial z} + \frac{\partial^2\psi}{\partial x^2} + \frac{\partial^2(\varphi_{P1} + \varphi_{P2})}{\partial z\partial x} - \frac{\partial^2\psi}{\partial z^2}\right], \tag{28}$$

where τ_{zx} is the shear stress of the porous media.

3.3. Interface between Patchy Saturated Porous Media and Elastic Solid (z = h)

(1) The continuity of the normal displacements of the porous media and the solid is given by

$$u_z = u'_z, \quad \frac{\partial\varphi_{P1}}{\partial z} + \frac{\partial\varphi_{P2}}{\partial z} + \frac{\partial\psi}{\partial x} = \frac{\partial\varphi_e}{\partial z} + \frac{\partial\psi_e}{\partial x}. \tag{29}$$

(2) The continuity of the normal displacements of the skeletal frame and the pore water is given by

$$w_z = 0, \quad \alpha_{P1}\frac{\partial\varphi_{P1}}{\partial z} + \alpha_{P2}\frac{\partial\varphi_{P2}}{\partial z} + \alpha_S\frac{\partial\psi}{\partial x} = 0. \tag{30}$$

(3) The continuity of the tangential displacement of the porous skeleton and the solid is given by

$$u_x = u'_x,$$
$$\frac{\partial\varphi_{P1}}{\partial x} + \frac{\partial\varphi_{P1}}{\partial x} - \frac{\partial\psi}{\partial z} = \frac{\partial\varphi_e}{\partial x} - \frac{\partial\psi_e}{\partial z}. \tag{31}$$

(4) The equilibrium of normal stress, $\tau_{zz} = \tau'_{zz}$, where τ'_{zz} is the normal stress of the solid and expressed as

$$\tau'_{zz} = (\lambda_e + 2\mu_e)\left(\frac{\partial^2\varphi_e}{\partial x^2} + \frac{\partial^2\varphi_e}{\partial z^2}\right) - 2\mu_e\left(\frac{\partial^2\varphi_e}{\partial x^2} - \frac{\partial^2\psi_e}{\partial x\partial z\partial x}\right). \tag{32}$$

(5) The equilibrium of the tangential stress, $\tau_{zx} = \tau'_{zx}$, where τ'_{zz} is the normal stress of the solid and expressed as

$$\tau'_{zx} = \mu_e\left(\frac{\partial u'_x}{\partial z} + \frac{\partial u'_z}{\partial x}\right) = \mu_e\left(2\frac{\partial^2\varphi_e}{\partial x\partial z} + \frac{\partial^2\psi_e}{\partial x^2} - \frac{\partial^2\psi_e}{\partial z^2}\right). \tag{33}$$

Combining Eqs. (14)-(20) and (28)–(36), we obtain the unknown constants B_r, A_{p1}, A_{p2}, A_s, B_{p1}, B_{p2}, B_s, A_{tp} and A_{ts} as follows:

$$[M][B_r \;\; A_{p1} \;\; A_{p2} \;\; A_s \;\; B_{p1} \;\; B_{p2} \;\; B_s \;\; A_{tp} \;\; A_{ts}]^T = A_i[B], \tag{34}$$

where A_i is the known constant, $[M]$ is a 9×9 matrix, and $[B]$ is a column matrix with nine elements. The elements of the matrices $[M]$ and $[B]$ can be found in the Appendix A.

4. NUMERICAL INVESTIGATION

Using the formulations derived in Section 3 the reflection coefficients B_r/A_i are investigated for several patchy saturated porous media cases. In the following numerical examples, the patchy saturated porous media will be investigated for low water saturation ($S_1 = 0.1$) and high water saturation ($S_1 = 0.9$) in gas-water model and oil-water model.

The parameters for the patchy saturated porous media are given in Table [28], the bulk modulus and density of the water are $K_w = 2.25$ GPa and $\rho_w = 1000$ kg/m^3, Lame's constants and density of the elastic solid substrate are $\lambda_e = 20.6$ GPa, $\mu_e = 14.2$ GPa and $\rho_e = 2460$ kg/m^3. The inside fluid patch radius $a = 0.01$ m. c is the consolidation parameter, it can be used for deducing drained bulk modulus K_D and drained shear modulus G [18] as follow:

$$K_D = K_s\frac{1-\varphi}{1+c\varphi},$$
$$G = G_s\frac{1-\varphi}{1+\frac{3}{2}c\varphi}. \tag{35}$$

Figure 2 shows the reflection coefficient in overlying water as a function of θ in the cases of different models, different water saturations and different porous media depths. When h is zero, i.e., porous media layer is absent, there are two critical angles. However, when the porous layer is present, there is not obvious critical angle result from the energy loss in porous media. In the case of thin porous media layer ($h = 1$ m), each reflection coefficient is lower than those observed when h is zero except for the low water saturation in gas-water model (Fig. 2a). In addition, the differences between $h = 0$ and $h = 1$ m in oil-water model are lower than the differences between $h = 0$ and $h = 1$ m in gas-water model (due to the very low value of the gas bulk modulus). With the increase of the porous media depth, reflection coefficient becomes more and more similar to the semi-infinite porous media case. That is to say, if the porous medium depth reaches some value, the effect of the underlying solid can be neglected.

Figure 3 shows that the reflection coefficient always oscillates with the increase of frequency. The resonant response of the $p1$-wave in the porous media leads to the oscillation of the reflection coefficient. In low frequency, the water saturation has little influence on the reflection coefficient no matter in the gas-water model (a) and the oil-water model (b). However, in high frequency, water saturation has a significant effect on the reflection coefficient in two models. Moreover, for the reflection coefficient, the differences between low gas (oil) saturation cases are higher than those between high gas (oil) saturation cases.

5. CONCLUSIONS

Reflection of elastic waves at an interface of water/patchy saturated porous media with underlying solid substrate is investigated based on the patchy saturation theory. The conclusions we summarize according to numerical results as follows. The differences between two patchy saturated porous media cases in oil-water model are lower than that between

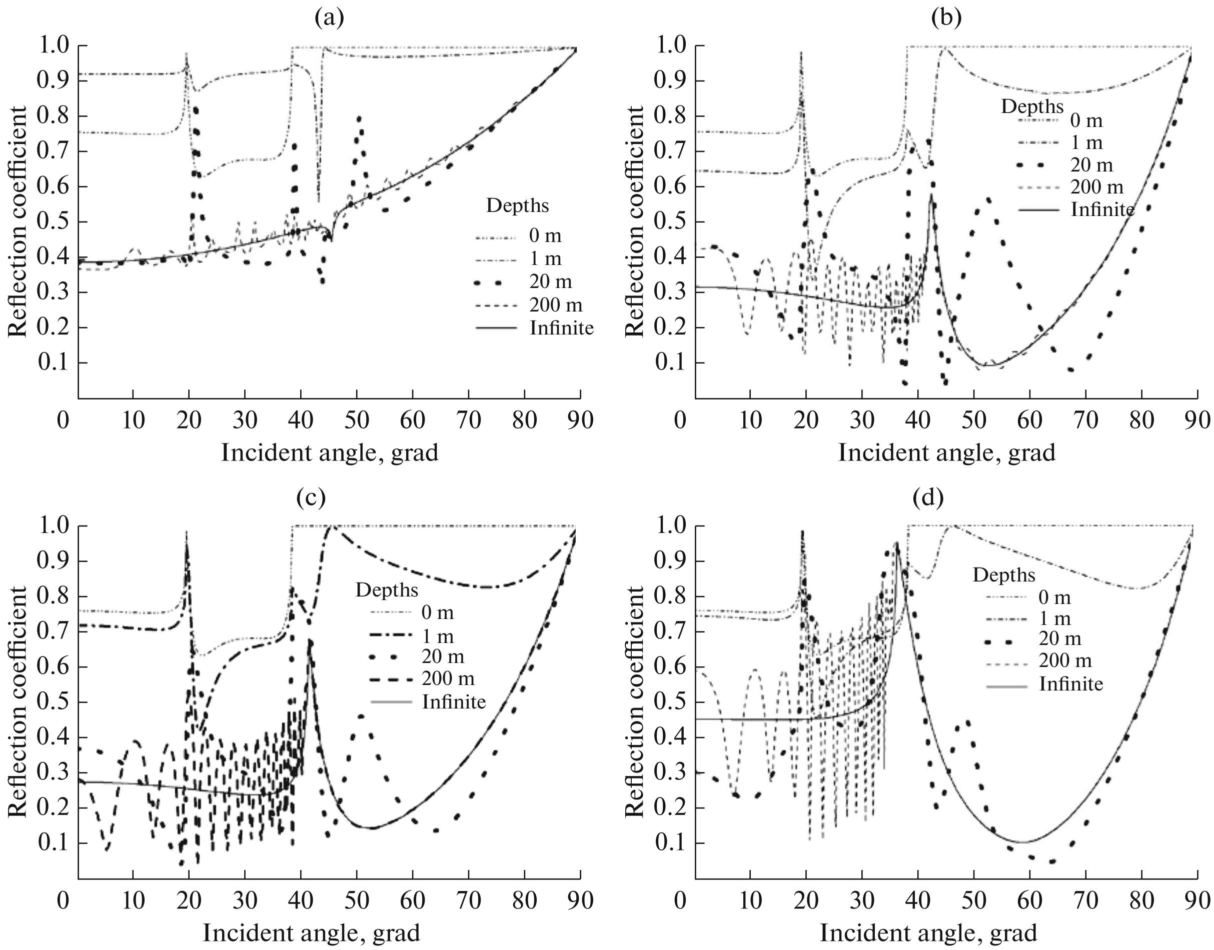

Fig. 2. Reflection coefficient varying with incident angle θ for gas-water model (a, b) and oil-water model (c, d) at $f = 100$ Hz and $h = 0$, 1, 20, 200 m and ∞. (a, c) $S_1 = 0.1$ and (b, d) $S_1 = 0.9$.

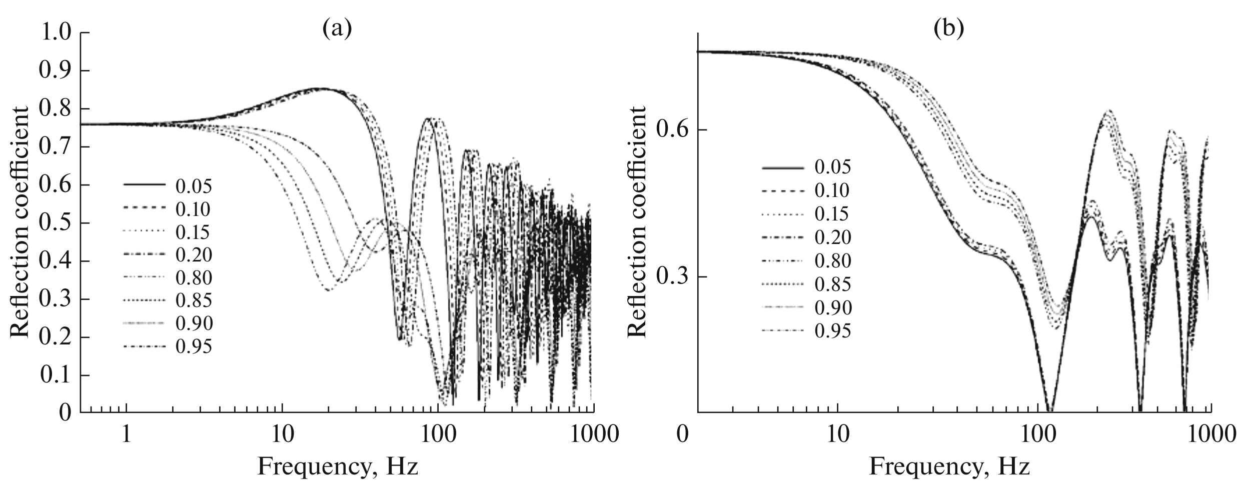

Fig. 3. Reflection coefficient varying with frequency f for gas-water model (a) and oil-water model (b) at $\theta = 0^\circ$ and $h = 5$ m.

Table 1. Model properties of the patchy saturated porous media

Solid skeletal frame	Bulk modulus of the solid matrix	K_s=40 GPa
	Shear modulus of the solid matrix	G_s = 42.7 GPa
	Density of solid matrix	ρ_s = 2690 kg/m^3
	Porosity	φ = 0.32
	Permeability	$\kappa = 9 \times 10^{-10}$ m^2
	Consolidation parameter	c = 18
	Biot–Willis constant	α = 0.1006
	Tortuosity	α_∞ = 1.0
Fluid 1 (water)	Bulk modulus	K_{f1} = 3.01 GPa
	Density	ρ_{f2} = 1055 kg/m3
	Viscosity	η_1 = 0.001 Pa s
Fluid 2 (gas)	Bulk modulus	K_{f2} = 0.13 GPa
	Density	ρ_{f2} = 336 kg/m^3
	Viscosity	η_2 = 0.00004 Pa s
Fluid 2 (oil)	Bulk modulus	K_{f2} = 1 GPa
	Density	ρ_{f2} = 750 kg/m^3
	Viscosity	η_2 = 0.001 Pa s

the same two cases in gas-water model. With the increasing frequency, the reflection coefficient always oscillates because of the resonant response of Biot's fast compressional wave. The water saturation has little influence on the reflection coefficient in two models at low frequency, and then it has a significant effect on the reflection coefficient at high frequency. Moreover, the curves are sensitive to water saturation in low gas (oil) saturation cases.

FUNDING

This work is supported by the National Natural Science Foundation of China under the contracts (nos. 41374147, 41474098, 11134011) and the Natural Science Foundation of Jilin Province of China (Grant no. 20180101282JC).

APPENDIX A

The elements of the matrix $[M]$ in Eq. (34) are given by:

$$M_{11} = \sigma_i, \quad M_{12} = (1+\alpha_{p1})\sigma_{p1},$$
$$M_{13} = (1+\alpha_{p2})\sigma_{p2}, \quad M_{14} = (1+\alpha_s)l_s,$$
$$M_{15} = -(1+\alpha_{p1})\sigma_{p1},$$

$$M_{16} = -(1+\alpha_{p2})\sigma_{p2},$$
$$M_{17} = (1+\alpha_s)l_s, \quad M_{18} = M_{19} = 0;$$

$$M_{21} = -\rho_w\omega^2,$$
$$M_{22} = M_{25} = (C(\omega) + M(\omega)\alpha_{p1})k_{p1}^2,$$
$$M_{23} = M_{26} = (C(\omega) + M(\omega)\alpha_{p2})k_{p2}^2,$$

$$M_{24} = M_{27} = M_{28} = M_{29} = 0;$$

$$M_{31} = \rho_w\omega^2, \quad M_{32} = M_{35} = 2G(\omega)l_{p1}^2$$
$$- (H(\omega) + C(\omega)\alpha_{p1})k_{p1}^2,$$

$$M_{33} = M_{36} = 2G(\omega)l_{p2}^2 - (H(\omega) + C(\omega)\alpha_{p2})k_{p2}^2,$$

$$M_{34} = -2G(\omega)l_s\sigma_s,$$
$$M_{37} = 2G(\omega)l_s\sigma_s, \quad M_{38} = M_{39} = 0;$$

$$M_{41} = 0, \quad M_{42} = -2l_{p1}\sigma_{p1}, \quad M_{43} = -2l_{p2}\sigma_{p2},$$
$$M_{44} = M_{47} = k_s^2 - 2l_s^2, \quad M_{45} = 2l_{p1}\sigma_{p1},$$

$$M_{46} = 2l_{p2}\sigma_{p2}, M_{48} = M_{49} = 0;$$

$$M_{51} = 0, \quad M_{52} = \sigma_{p1}e^{i\sigma_{p1}h}, \quad M_{53} = \sigma_{ps}e^{i\sigma_{p2}h},$$
$$M_{54} = l_s e^{i\sigma_s h}, \quad M_{55} = -\sigma_{p1}e^{-i\sigma_{p1}h},$$

$$M_{56} = -\sigma_{p2}e^{-i\sigma_{p2}h}, \quad M_{57} = l_s e^{-i\sigma_s h},$$
$$M_{58} = -\sigma_{tp}e^{i\sigma_{tp}h}, \quad M_{59} = -l_{ts}e^{i\sigma_{ts}h};$$

$$M_{61} = 0, \quad M_{62} = \alpha_{p1}\sigma_{p1}e^{i\sigma_{p1}h},$$
$$M_{63} = \alpha_{p2}\sigma_{p2}e^{i\sigma_{p2}h}, \quad M_{64} = \alpha_s l_s e^{i\sigma_s h},$$
$$M_{65} = -\alpha_{p1}\sigma_{p1}e^{-i\sigma_{p1}h},$$
$$M_{66} = -\alpha_{p2}l_{p2}e^{-i\sigma_{p2}h}, \quad M_{67} = \alpha_s l_s e^{-i\sigma_s h},$$
$$M_{68} = 0, M_{69} = 0;$$
$$M_{71} = 0, \quad M_{72} = l_{p1}e^{i\sigma_{p1}h}, \quad M_{73} = l_{p2}e^{i\sigma_{p2}h},$$
$$M_{74} = -\sigma_s e^{i\sigma_s h}, \quad M_{75} = l_{p1}e^{-i\sigma_{p1}h},$$
$$M_{76} = l_{p2}e^{-i\sigma_{p2}h}, \quad M_{77} = \sigma_s e^{-i\sigma_s h},$$
$$M_{78} = -l_{tp}e^{i\sigma_{tp}h}, \quad M_{79} = \sigma_{ts}e^{i\sigma_{ts}h};$$
$$M_{81} = 0, \quad M_{82} = (2G(\omega)l_{p1}^2 - (H(\omega) + C(\omega)\alpha_{p1})k_{p1}^2)e^{i\sigma_{p1}h},$$
$$M_{83} = (2G(\omega)l_{p2}^2 - (H(\omega) + C(\omega)\alpha_{p2})l_{p2}^2)e^{i\sigma_{p2}h},$$
$$M_{84} = -2G(\omega)l_s\sigma_s e^{i\sigma_s h},$$
$$M_{85} = (2G(\omega)l_{p1}^2 - (H(\omega) + C(\omega)\alpha_{p1})l_{p1}^2)e^{-i\sigma_{p1}h},$$
$$M_{86} = (2G(\omega)l_{p2}^2 - (H(\omega) + C(\omega)\alpha_{p2})k_{p2}^2)e^{-i\sigma_{p2}h},$$
$$M_{87} = 2G(\omega)l_s\sigma_s e^{-i\sigma_s h},$$
$$M_{88} = \left(\lambda_e k_{tp}^2 + 2\mu_e\sigma_{tp}^2\right)e^{i\sigma_{tp}h},$$
$$M_{89} = 2\mu_e l_{ts}\sigma_{ts}e^{i\sigma_{ts}h};$$
$$M_{91} = 0, \quad M_{92} = -2G(\omega)l_{p1}\sigma_{p1}e^{i\sigma_{p1}h},$$
$$M_{93} = -2G(\omega)l_{p2}\sigma_{p2}e^{i\sigma_{p2}h},$$
$$M_{94} = G(\omega)(k_s^2 - 2l_s^2)e^{i\sigma_s h},$$
$$M_{95} = 2G(\omega)l_{p1}\sigma_{p1}e^{-i\sigma_{p1}h},$$
$$M_{96} = 2G(\omega)l_{p2}\sigma_{p2}e^{-i\sigma_{p2}h},$$
$$M_{97} = G(\omega)(k_s^2 - 2l_s^2)e^{-i\sigma_s h},$$
$$M_{98} = 2\mu_e l_{tp}\sigma_{tp}e^{i\sigma_{tp}h},$$
$$M_{99} = -\mu_e(k_{ts}^2 - 2l_{ts}^2)e^{i\sigma_{ts}h};$$

where k_{p1}, k_{p2}, k_s and k_{tp}, k_{ts} are the wave numbers of the $p1$-, $p2$-, S-waves in the porous media and P-, S-waves in the solid, respectively. They are given by

$$k_{p1}^2 = l_{p1}^2 + \sigma_{p1}^2, \quad k_{p2}^2 = l_{p2}^2 + \sigma_{p2}^2,$$
$$k_s^2 = l_s^2 + \sigma_s^2, \quad k_{tp}^2 = l_{tp}^2 + \sigma_{tp}^2,$$
$$k_{ts}^2 = l_{ts}^2 + \sigma_{ts}^2.$$

The matrix $[B]$ in Eq. (48) are given by

$$[B] = \left[\sigma_i \;\; \rho_w\omega^2 \;\; -\rho_w\omega^2 \;\; 0 \;\; 0 \;\; 0 \;\; 0 \;\; 0 \;\; 0\right]n^T.$$

REFERENCES

1. R. D. Stoll and T. K. Kan, J. Acoust. Soc. Am. **70** (S1), 149 (1981).
2. Z. W. Cui and K. X. Wang, Int. J. Eng. Sci. **41** (18) 2179 (2003).
3. M. Tajuddin and S. J. Hussaini, J. Appl. Geophys. **58**, 59 (2006).
4. M. G. Markov, Acoust. Phys. **51**, S115 (2005).
5. M. G. Markov, Acoust. Phys. **52** (4), 429 (2006).
6. M. G. Markov, Izv., Phys. Solid Earth **45** (9), 769 (2009).
7. S. Z. Dunin and V. N. Nikolaevskii, Acoust. Phys. **51**, S61 (2005).
8. V. N. Nikolaevskii and G. S. Stepanova, Acoust. Phys. **51**, S131 (2005).
9. Z. J. Dai, Z. B. Kuang, and S. X. Zhao, Int. J. Rock Mech. Min. Sci. **43**, 961 (2006).
10. J. T. Wang, F. Jin, and C. H. Zhang, Ocean Eng. **63**, 8 (2013).
11. D. D. Lyu, J. T. Wang, F. Jin, and C. H. Zhang, Transp. Porous Media **103**, 25 (2014). https://doi.org/10.1007/s11242-014-0286-7
12. W. Y. Chen, Z. H. Wang, K. Zhao, G. Chen, and X. J. Li, Geophys. J. Int. **203**, 213 (2015).
13. N. C. Dutta and H. Odé, Geophysics **44**, 1777 (1979).
14. N. C. Dutta and H. Odé, Geophysics **44**, 1789 (1979).
15. N. C. Dutta and A. J. Seriff, Geophysics **44**, 1806 (1979).
16. G. A. Gist, Geophysics **59**, 1100 (1994).
17. D. L. J. Johnson, Acoust. Soc. Am. **110** (2), 682 (2001). https://doi.org/10.1121/1.1381021
18. S. R. Pride, *Hydrogeophysics,* Ed. by Y. Rubin and S. Hubbard (Springer, 2005), p. 253.
19. S. R. Pride, J. G. Berryman, and J. M. J. Harris, Geophys. Res. **109**, B01201 (2004). https://doi.org/10.1029/2003JB002639
20. A. N. Norris, J. Acoust. Soc. Am. **94**, 359 (1993). https://doi.org/10.1121/1.407101
21. A. A. Abrashkin, V. S. Averbakh, S. N. Vlasov, Yu. M. Zaslavskii, I. A. Soustova, R. A. Sudarikov, and Yu. I. Troitskaya, Acoust. Phys. **51**, S12 (2005).
22. S. K. Tomar and A. Arora, Int. J. Solids Struct. **43**, 1991 (2006).
23. K. Tuncay and M. Y. J. Corapcioglu, Appl. Mech. **64**, 313 (1997).
24. B. Quintal, S. M. Schmalholz, and Y. Y. Podladchikov, Geophysics **76** (2), N1 (2001).
25. T. M. Müller and B. Gurevich, Geophysics **69**, 1166 (2004). https://doi.org/10.1190/1.1801934
26. T. M. Müller, B. Gurevich, and M. Lebedev, Geophysics **75** (5), 75A147 (2010).
27. J. Toms, T. M. Müller, and B. Gurevich, Geophys. Prospect **55** (5), 671 (2007).
28. B. Dupuy and A. Stoves, Geophysics **79** (1), B19 (2014).